

Dislocation Dynamics

Dorn, Mitchel and Hauser (1965)

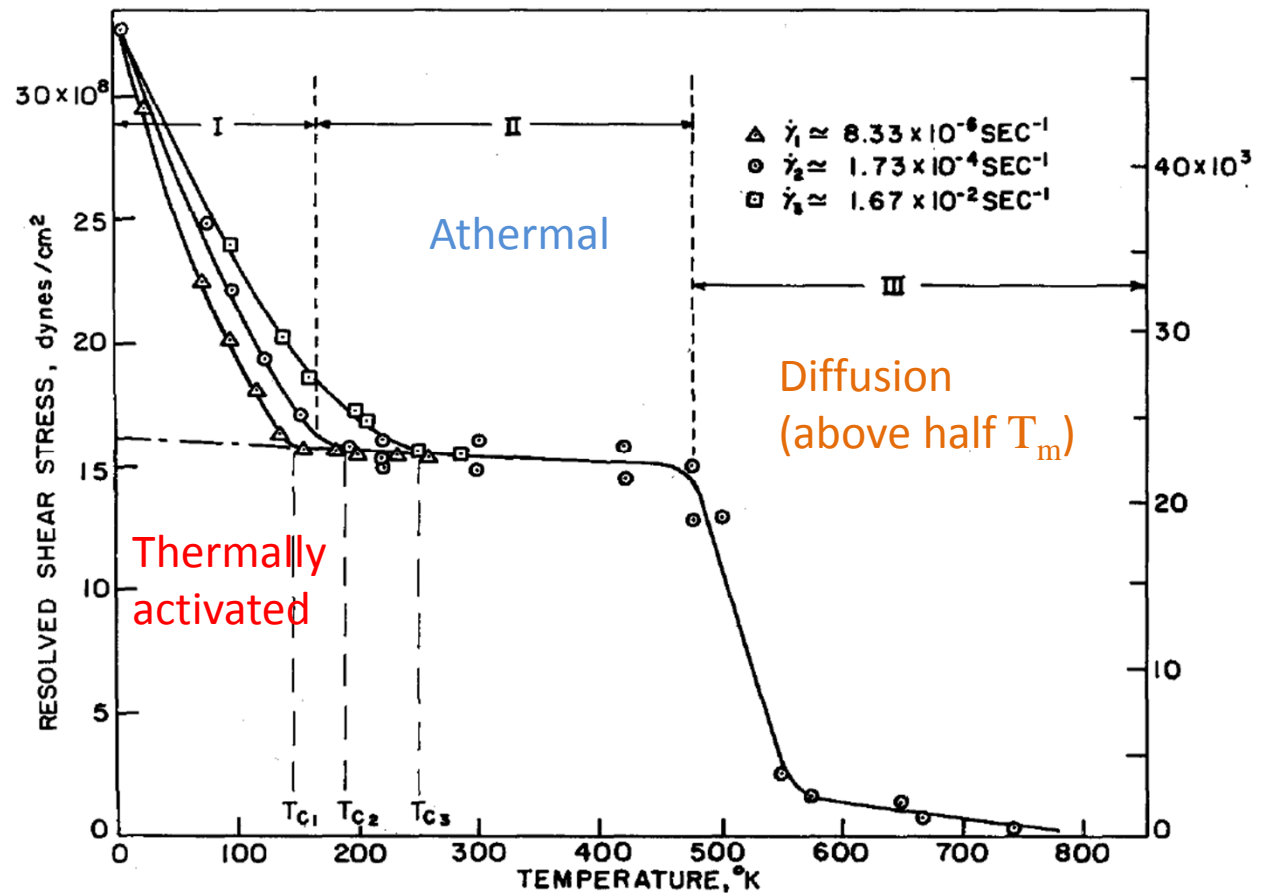
Review dislocation mechanisms:

Athermal

Thermally activated

High-velocity damping

Relativistic effects

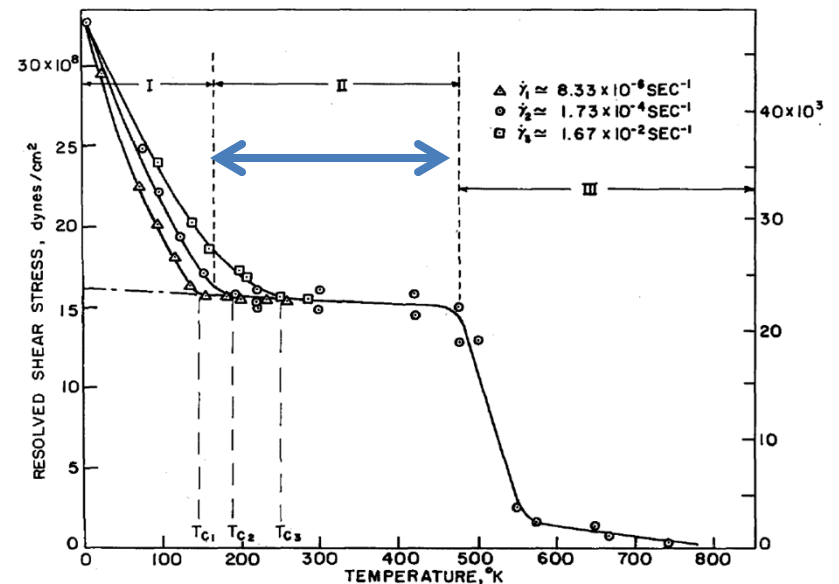


Effect of temperature on CRSS for prismatic slip of Ag 33at.% Al single crystal

Athermal Mechanisms

- Yield stress decreases slightly with T (so does shear modulus G)
- Yield stress independent of strain rate
- von Karman assumption that deformation stress is only a function of strain is good

- Surmounting long range stress field
- Breaking attractive junctions (x functions)
- Overcoming strong-solute atom locking
- ...



Thermally Activated Mechanisms

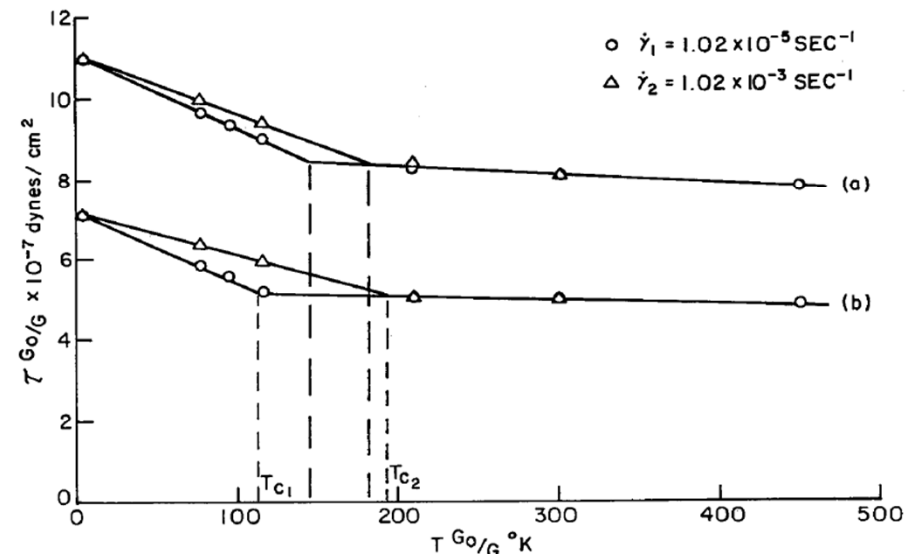
- When barriers are **localized** and **not too high**
- Yield stress depends on T and strain rate
- T_c increase with strain rate

$$\tau = \tau_A + \frac{U_j}{Lb^2} - \frac{kT}{Lb^2} \ln \left\{ \frac{NAb^2\nu_0}{L\dot{\gamma}} \right\} \quad T \leq T_c$$

$$\tau = \tau_A \quad T \geq T_c$$

$$\tau_A = \tau_{A0} G/G_0$$

- Intersection (forest dislocation)
- Peierls mechanism (kink pair)
- Cross slip
- Solute atom
- Diffusion controlled mechanisms



Effect of temperature on flow stress of Al single crystal at two pre-strains

Kink Pair Nucleation Mechanism

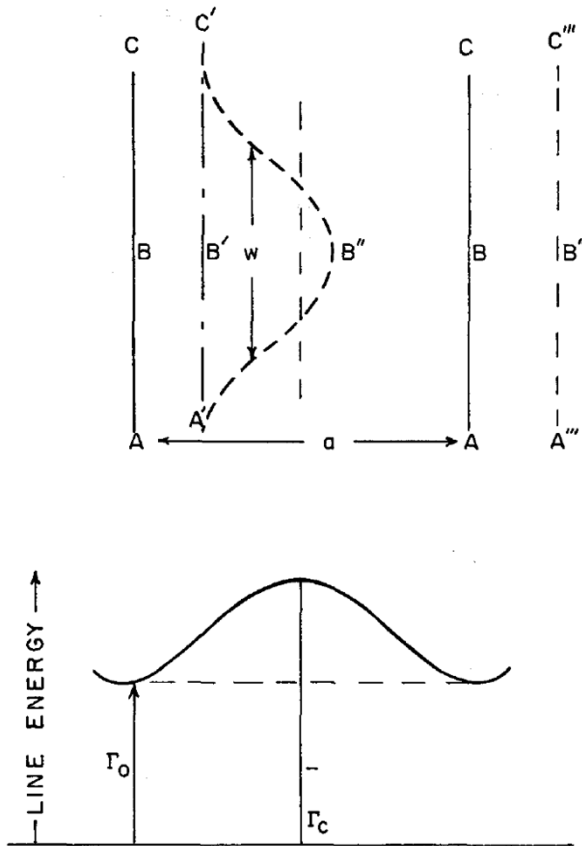


Fig. 4—Nucleation of a pair of dislocation kinks in the Peierls process

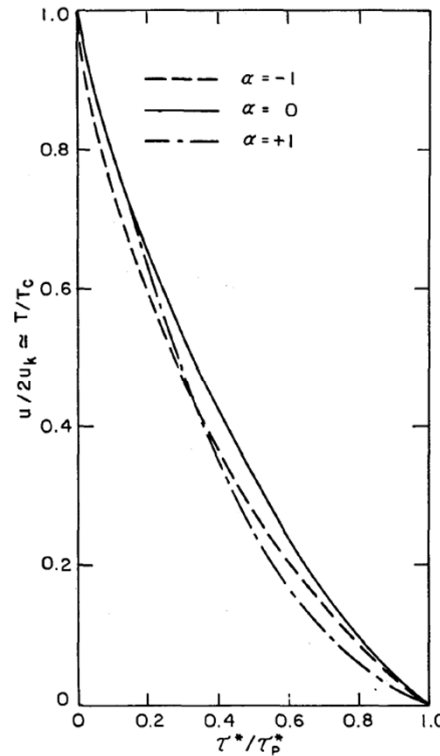


Fig. 5—Effect of stress on the activation energy for kink nucleation

$$v = \frac{\nu a L}{w} e^{-U_n/kT} \quad T \leq T_c$$

$$\dot{\gamma} = \frac{\rho b a L v}{w} e^{-U_n/kT} \quad T \leq T_c$$

$$\dot{\gamma} = \frac{\rho b a L v}{w} e^{-2U_k/kT_c} \quad \text{At } T_c$$

High-velocity Damping

- When stress exceeds $\tau^* + \tau_A$

$$(\tau - \tau_B) \simeq \frac{CvT}{25c} \frac{\dot{\gamma}}{\rho b} = \frac{CvT \sqrt{3}\dot{\epsilon}}{25c\rho b}$$

- Thermoelastic
(local T change as dislocation move)
- Phonon viscosity
(change of phonon modes)
- Anharmonic damping
(non-linear dislocation core)
- Phonon scattering
(by disl stress field, by disl vibration)

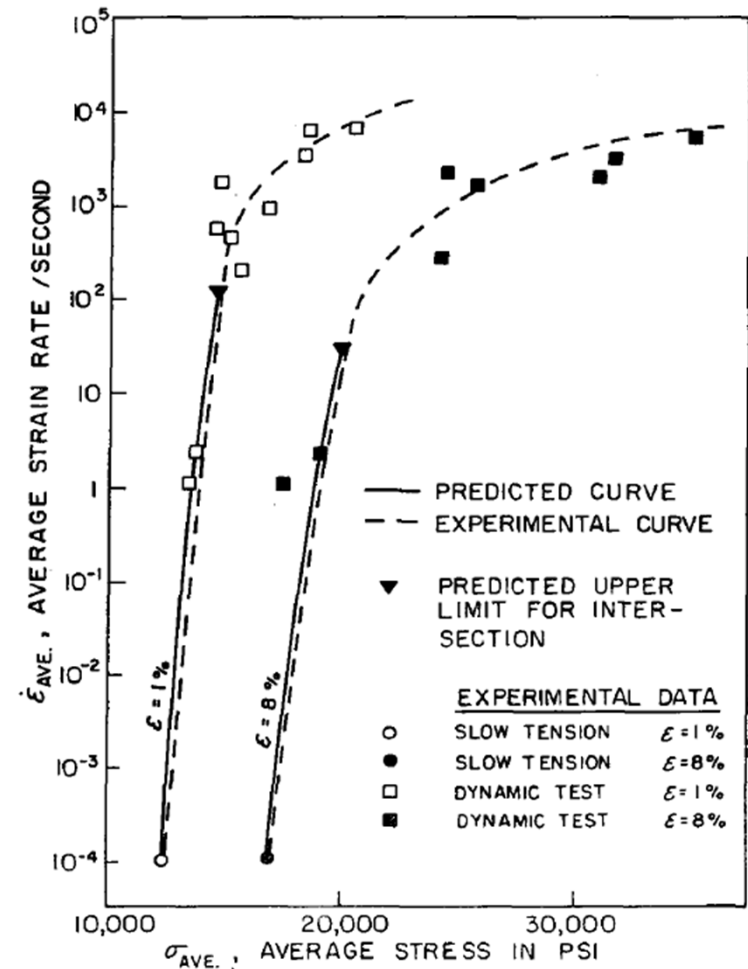


Fig. 7a—Prediction of the dynamic plastic behavior in the intersection region for pure Al at $T = 77^\circ\text{K}$

Relativistic Effects

- Line energy of screw dislocation

$$\Gamma = \Gamma_0 / \left\{ 1 - \left(\frac{v}{c} \right)^2 \right\}^{1/2}$$

- Experimental verification difficult

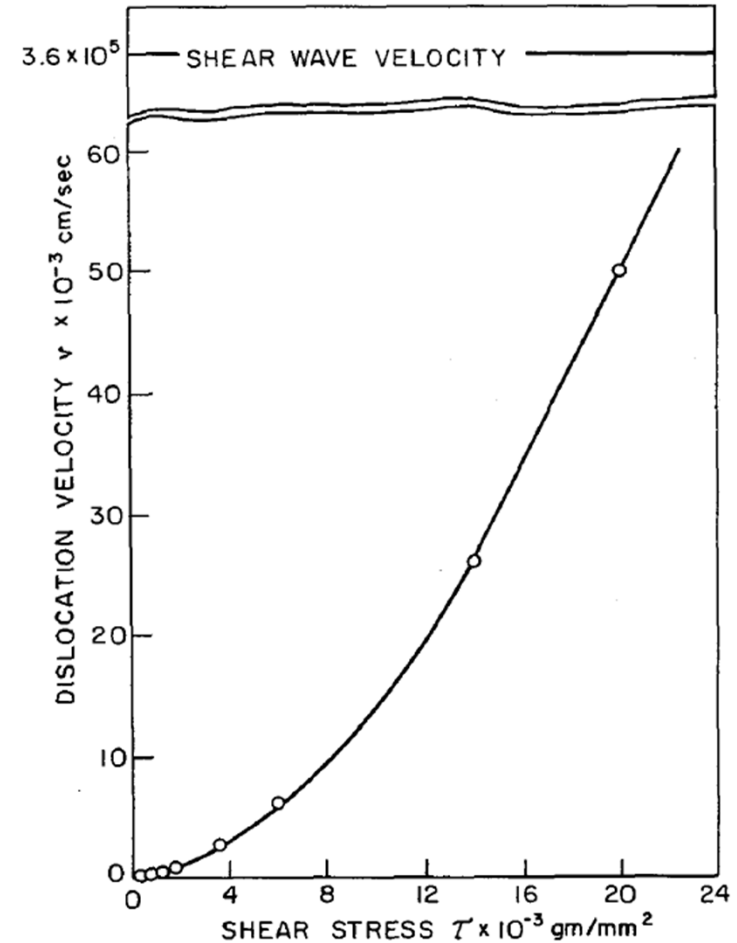


Fig. 8b—Edge-dislocation velocity vs. resolved shear stress for LiF²⁰

Dislocation Mobility Data

$$F = (\tau - \tau_B)b = Bv \quad (20)$$

B is drag coefficient

M = B⁻¹ is mobility

τ in unit of 1 = dynes/cm² = 0.1 Pa

B in unit of 0.1 Pa·s

TABLE 4—DISLOCATION-DAMPING COEFFICIENTS [B of eq (20)]

Material	LiF	NaCl	KCl	Quartz	Cu	Cu-0.13% Mn
Observed Values						
Dislocation-velocity measurements	$7 \times 10^{-4(30)}$	$2 \times 10^{-4(31)}$				
Acoustical-attenuation measurements	$1.3 \times 10^{-3(38)}$	$2 \times 10^{-3(40)}$	$3.5 \times 10^{-4(38)}$	$6 \times 10^{-4(24)}$	$6 \times 10^{-5(24)}$ $7.9 \times 10^{-5(38)}$ $8 \times 10^{-4(41)}$ $6.5 \times 10^{-4(42)}$	$4.5 \times 10^{-4(38)}$
Theoretical Values						
Thermoelastic	$1.7 \times 10^{-4(24)}$	$7.1 \times 10^{-5(24)}$ $7.7 \times 10^{-5(38)}$		$2.5 \times 10^{-5(24)}$	$1 \times 10^{-5(24)}$	
Phonon viscosity	$9 \times 10^{-4(24)}$ $4.5 \times 10^{-5(38)}$	$2.1 \times 10^{-3(24)}$ $1.1 \times 10^{-4(38)}$	$1.9 \times 10^{-4(38)}$	$6 \times 10^{-4(24)}$	$5 \times 10^{-5(24)}$ $7 \times 10^{-5(38)}$	$1 \times 10^{-4(38)}$
Phonon scattering	$5.6 \times 10^{-5(24,38)}$	$7.7 \times 10^{-5(24)}$	$5.9 \times 10^{-5(38)}$	$4 \times 10^{-5(24)}$	$1 \times 10^{-4(24)}$ $1.1 \times 10^{-4(38)}$	$9 \times 10^{-5(38)}$